Highly Efficient IGFC Hybrid Power Systems Employing Bottoming Organic Rankine Cycles With Optional Carbon Capture

R. J. Braun
Engineering Division,
Colorado School of Mines,
Golden, CO 80401

S. Kameswaran

J. Yamanis

E. Sun

United Technologies Research Center,
East Hartford, CT 06108

This study examines the performance of a solid oxide fuel cell- (SOFC-) based integrated gasification power plant concept at the utility scale (>100 MW). The primary system concept evaluated was a pressurized ~150 MW SOFC hybrid power system integrated with an entrained-flow, dry-fed, oxygen-blown, slagging coal gasifier and a combined cycle in the form of a gas turbine and an organic Rankine cycle (ORC) power generator. The analyzed concepts include carbon capture via oxy-combustion followed by water knockout and gas compression to pipeline-ready CO_2 sequestration conditions. The results of the study indicate that hybrid SOFC systems could achieve electric efficiencies approaching 66% [lower heating value (LHV)] when operating fueled by coal-derived clean syngas and without carbon dioxide capture. The system concept integrates SOFCs with the low-pressure turbine spool of a 50 MW Pratt & Whitney FT8-3 TwinPak gas turbine set and a scaled-up, water-cooled 20 MW version of the Pratt & Whitney (P&W) PureCycle ORC product line (approximately 260 kW). It was also found that a system efficiency performance of about 48% (LHV) is obtained when the system includes entrained-flow gasifier and carbon capture using oxygen combustion. In order to integrate the P&W FT8 into the SOFC system, the high-pressure turbine spool is removed which substantially lowers the FT8 capital cost and increases the expected life of the gas turbine engine. The impact of integrating an ORC bottoming cycle was found to be significant and can add as much as 8 percentage points of efficiency to the system. For sake of comparison, the performance of a higher temperature P&W ORC power system was also investigated. Use of a steam power cycle, in lieu of an ORC, could increase net plant efficiency by another 4%, however, operating costs are potentially much lower with ORCs than steam power cycles. Additionally, the use of cathode gas recycle is strongly relevant to efficiency performance when integrating with bottoming cycles. A parameter sensitivity analysis of the system revealed that SOFC power density is strongly influenced by design cell voltage, fuel utilization, and amount of anode recycle. To maximize the power output of the modified FT8, SOFC fuel utilization should be lower than 70%. Cathode side design parameters, such as pressure drop and temperature rise were observed to only mildly affect efficiency and power density. [DOI: 10.1115/1.4004374]

1 Introduction

Solid oxide fuel cells (SOFCs) are considered to be a key technology for high-efficiency, zero-emission fossil power plants of the future. In particular, the accelerating development activity of SOFCs under the auspices of the U.S. DOE Solid State Energy Conversion Alliance (SECA) program is focused on utilizing SOFCs as building blocks for large-scale integrated coal-gasification power plants. When SOFCs are fueled from coal syngas and combined with gas turbines, an ultra-high efficiency hybrid system can be obtained. A steam Rankine bottoming cycle (SRC) can also be integrated to further enhance efficiency and power production and carbon dioxide capture and sequestration (CCS) is necessary to achieve near-zero emission levels. It has been estimated that an integrated gasification fuel cell (IGFC) power plant with CCS can achieve an efficiency advantage of nearly 24 percentage points over a comparable integrated gasification combined cycle plant with CCS [1].

There are numerous challenges in integrating the many subsystems that comprise an IGFC power plant. Achieving robust operability and control and a flexible operating envelope in a cost-effective manner are significant concerns for hybrid power systems, especially those involving numerous unproven technologies. Technical challenges include gasifier-fuel cell integration, fuel cell-gas turbine integration, power block integration with carbon capture hardware, and system control. Gasifier-fuel cell integration is subject to the very narrow operating envelope of SOFC technology established by both tolerance to anode fuel gas impurities, and cell-stack temperature and pressure control. Excursions of reactant gas temperatures, pressures, and compositions from design conditions can lead to cell cracking, carbon deposition, anode oxidation, and accelerated cell degradation (reduced lifetime). Fuel cell-gas turbine integration is subject to the same SOFC operating constraints as gasifier integration and is further hampered by several control challenges that involve compressor surge, shaft overspeed, and cell overheating [2]. Detailed examination of the integration challenges

Contributed by the International Gas Turbine Institute (IGTI) for publication in the JOURNAL OF ENGINEERING FOR GAS TURBINES AND POWER. Manuscript received June 18, 2010; final manuscript received May 18, 2011; published online December 14, 2011. Assoc. Editor: Paolo Chiesa.

is beyond the scope of this paper, but the interested reader is referred to several literature studies on the topic [2–9].

Despite the numerous technical challenges that need to be overcome, both the efficiency performance and the economics of "mature" IGFC systems are promising. Recent economic assessments of large-scale (>100 MW) integrated gasification combined cycle (IGCC) plants employing entrained-flow gasifiers and F-class syngas turbines have estimated total plant capital costs at about $1800/kW[1] (in 2007$) using commercially available technologies without carbon capture [1,10]. It is estimated that capturing carbon dioxide in these plants adds another 30% to the total plant capital cost [1]. In contrast, the cost of an IGFC plant that employs catalytic gasifier technology and carbon capture has been estimated to reduce the plant capital cost by 30% (i.e., ~$1670/kW) while offering an efficiency advantage of nearly 24 percentage points over its IGCC/CCS counterpart [1]. Such cost and performance advantages make IGFC/CCS systems very attractive; however, considering the substantial technical challenges of realizing these performance expectations, continued exploration of system integration concepts is warranted.

The objectives of the present work are to (1) quantify IGFC system performance using commercial coal gasifier, gas turbine, and organic Rankine cycle (ORC) technologies, (2) perform a sensitivity study of system performance due to variations in SOFC power block design parameters, and (3) identify additional areas for system design and performance improvements.

There are several prior theoretical research efforts in the open literature that have examined integrating SOFCs with coal gasification and power generation cycles. In particular, Lobachyov and Richter evaluated integrating an indirectly heated fluidized-bed coal gasifier with gas turbine and SOFC [11]. Efficiencies exceeding 60%-LHV were reported with generic gas turbine and obsolete monolithic SOFC technologies and no carbon capture. Kivisaari et al., [12] examined integration of an entrained-flow gasifier with either molten carbonate or solid oxide fuel cell technology for combined heat and power (CHP). In this study, integration with power cycles was not performed nor was CO_2 capture of interest. Similarly, Ghosh and De carried out a study on employing entrained-flow gasification with SOFCs; however, gas and steam turbine integration for CHP were also incorporated [13]. Verma et al., [14] performed an analysis on IGFC systems inclusive of a steam cycle, ion transport membrane, and carbon capture technologies. SOFC parameter and system conceptual design variations were studied and efficiencies as high as 50%-HHV were reported. More recently, Romano et al., examined an IGFC system operating with an oxygen-blown, entrained-flow Shell gasifier [15]. The study details the integration of gasifier and power block islands, but does not offer carbon capture and sequestration. A sensitivity analysis of SOFC pressure and fuel and oxidant utilizations is given. Results of a 7–11 percentage point efficiency gain over advanced IGCC systems are reported. Liese reported on an IGFC system performance with pre- and post-SOFC carbon capture for a hybrid system employing a Conoco-Philips gasifier and a bottoming steam Rankine cycle [16]. The focus of this study was on the impact of various carbon capture methods. IGFC studies that employ low-temperature catalytic gasification have also been made [17,18]. These studies show even more promising efficiency performance potential of IGFC hybrid systems in part due to the methane content of gasifier syngas and the associated benefit to the SOFC power block. In terms of SOFC-ORC hybrid systems, Verda performed an integration study with a natural gas fueled commercial-scale tubular SOFC system of about 100 kW and a 30 kW ORC system [19]. Results point to a 5.6% efficiency improvement from the addition of the bottoming ORC system.

[1]This cost reflects an overnight installed capital cost that can be 50% lower than actual turn-key plant cost.

2 Methodology

The focus of the present work is on the performance assessment associated with the system integration of gas turbine and Rankine cycle hardware with that of the SOFC power block and presumes challenges associated with gasifier-SOFC/GT integration and overall system control have been overcome. In this paper, we examine the expected performance of an IGFC power plant when the SOFC power section is integrated with modified and/or scaled-up commercial gas turbine and ORC power generation technology. A schematic overview of the main process steps of a coal-based IGFC hybrid system with ORC and post-combustion CO_2 capture is given in Fig. 1. The first step of the IGFC system is production of a syngas through gasification of the coal feedstock. The coal is fed into the high-pressure gasifier using nitrogen as an inert pressurizing agent that is supplied from the air separation unit. Syngas cleanup and cooling occur next before admittance into the SOFC power block. In one sense, the IGFC system is very similar to its more conventional integrated gasification combined cycle (IGCC) counterpart in that the SOFC serves as a combustor that also produces electric power. Thus, the compressor of the gas turbine supplies air to the SOFC unit and the heat gain of the cathode air from the SOFC processes is returned to the turbine. The depleted anode tail-gas is kept separate from the cathode gases and is sent to the oxycombustor where the remaining fuel gas is combusted. Thermal energy is recovered from both gas turbine and oxycombustor exhaust gases via the ORC bottoming cycle. Carbon dioxide is separated in the final stage of the plant process as shown in Fig. 1. While an ORC bottoming cycle offers lower efficiency than a conventional steam cycle given the availability of the relatively high temperature heat sources in the IGFC system, there are potential cost benefits associated with integration of an ORC system that merit further exploration of its potential use. Further discussion is given in the subsequent section of this paper.

Integrated coal-gasification fuel cell power plant concepts have been investigated using modeling and simulation. The plant concepts evaluated feature entrained-flow gasifiers integrated with planar SOFC technology, Pratt & Whitney gas turbines, carbon capture via oxy-combustion of the anode tail-gas, and waste heat recovery through organic Rankine cycle systems. Physics-based component models and diagnostic tools previously developed at UTC facilitate fast prototyping of innovative fuel cell, turbine, and combined heat and power system configurations. The current system-level models have been generated employing zero-dimensional thermodynamic component models.

A viable system configuration was first established and sizing of the SOFC power block was derived from matching of reactant flows to the P&W FT8 gas turbine requirements. Design parameters were then varied to gauge performance sensitivity. Key parameters and the ranges explored are summarized in Table 1. Bounds for the range were constrained by hardware performance characteristics, such as maximum SOFC outlet temperature, or flow and compressor pressure ratios for the gas turbine spool.

3 Technologies

System technologies employed in the integrated gasification fuel cell power plant concept designs are briefly described below.

3.1 Coal Gasifier. The gasifier employed in the IGFC system analysis is a dry-fed oxygen-blown, entrained-flow slagging gasifier representative of Shell gasifier technology. It was assumed that the cold-gas gasifier efficiency (defined as LHV syngas out over LHV coal feed in) was 82% [20]. In this study, the focus was on effective integration of the prime movers, and thus gasifier and syngas cleanup sub-systems were not integrated with the SOFC-combined cycle power block. All steam generation needs for the gasifier and gas cleanup unit operations are generated by syngas process cooling needs, which can exceed the thermal energy

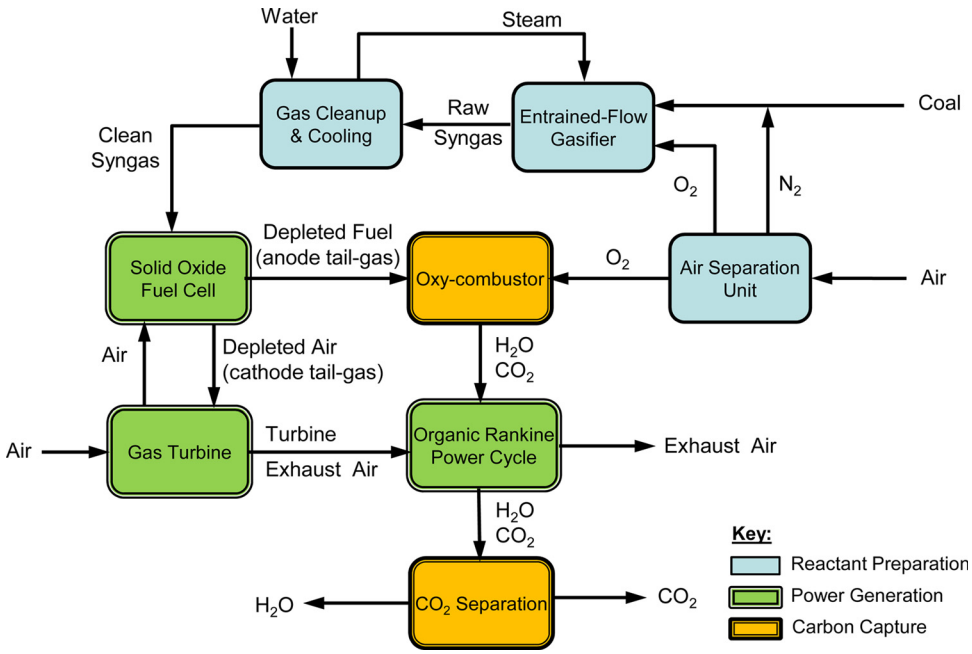

Fig. 1 Schematic overview of coal-based IGFC hybrid system with ORC and post-combustion CO_2 capture

Table 1 Parameters for system-level sensitivity study

Parameter	Range
System operating pressure	3–5 bar
Nominal SOFC operating temperature	775 °C (fixed)
Allowable cathode air temperature rise	75–150 °C
SOFC cathode pressure drop	2–10 kPa
SOFC fuel utilization	66–86%
SOFC average single cell voltage	0.68–0.79 V/cell

required for steam generation by as much as 250%. Thus, while such integration considerations are not a focus of the current study, auxiliary power requirements in the gasifier and cleanup operations could easily be met with expanders or larger ORC capacity. The excess process heat that is available could be employed to drive an ORC or SRC system and produce additional power thereby, increasing system efficiency. The potential reduction in system efficiency is estimated[2] at 1–2 percentage points from lack of tight thermal integration with power block and syngas production and cleanup unit operations, making the performance predictions given in the forthcoming sections more conservative.

3.2 SOFC Technology. The solid oxide fuel cell stack is based on planar cell technology that achieves performance levels consistent with DOE SECA performance targets, such as power density and cathode temperature rise. The "high performance" cell technology is based on a porous nickel yttria-stabilized zirconia (YSZ) anode support, a dense YSZ electrolyte membrane (~10 μm) and a porous strontium-doped lanthanum cobalt ferrite (LSCF) cathode electrode. The cell and the balance-of-stack components are optimized for 40 000 h durability. The stack power section is assumed to operate at low (3 kPa) pressure drops on both the anode and cathode gas streams in order to minimize parasitic power loss. The stack design and the stack arrangement for MW-scale power plants can be tailored to operate under near ambient (~1.0 bar) or elevated pressures (~5 bar). The anode-supported SOFC technology employed in this study typically operates in the 750–775 °C range with a maximum cathode outlet temperature of 850 °C, and with a cell power density of 0.45 W/cm^2 on syngas.

3.3 Gas Turbine. The gas turbine technology utilized in this study is based on the Pratt & Whitney FT8 Twin PAC 50 MW power system. It is comprised of two-single 25 MW, 37%-LHV efficiency (on natural gas) systems coupled to a single generator. The FT8 POWERPAC single-engine 25 MW gas turbine from Pratt & Whitney Power Systems is a 3600-rpm machine employed for 60 Hz electric power generation and has demonstrated operation in combined cycle (GT/steam Rankine cycle).

Figure 2 shows a simplified schematic of an aeroderivative gas turbine power generator. The engine is mainly comprised of a low-pressure compressor, high-pressure spool (compressor, turbine, and shaft), low-pressure turbine, power turbine, and synchronous 60 Hz generator. The low-pressure compressor typically develops a pressure ratio of 4.5, but can go as high as 5.2 bar. The high-pressure spool employs a concentric shaft and includes high-pressure compressor, diffuser, combustor, and high-pressure turbine components. The high-pressure spool operates at a speed greater than the low-pressure spool and the operating pressure of the combustor is typically on the order of 18–19 bar. As the SOFC design operating pressure is 5 bar, removal of the high-pressure

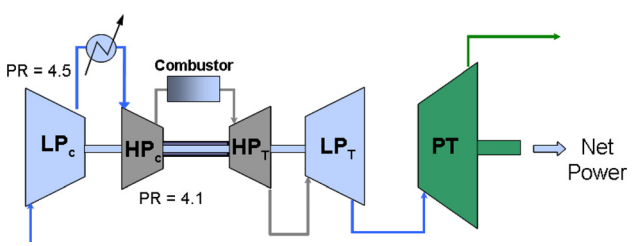

Fig. 2 Simplified schematic diagram of PW FT8-series gas turbine power generator

[2]The estimation is made by taking the 250% excess process thermal energy and generating power through either ORC or SRC power cycles at the efficiencies employed in this analysis.

spool of turbine when integrating with the SOFC is required. One of the challenges in matching a gas turbine power generator with an IG-SOFC topping plant is in the potential flow mismatch between compressor and expander due to the use of the low-calorific coal syngas in the system. When the SOFC capacity is selected to match the design flow rate and pressure ratio (PR) of the low-pressure compressor (LPC) section of the FT8 gas turbine product line, the mass flow delivered to the low-pressure turbine (LPT) section is too large for the unit. Another challenge is that since the high-pressure spool has been removed, the required inlet pressure to the low-pressure turbine is 2 bar higher than the outlet pressure available from the low-pressure compressor. Thus, removal of the high pressure spool presents an off-design aerodynamic inlet condition, even in cases where the compressor and turbine flowrates are properly matched. If the mismatch in either flow and pressure ratio are large enough, significant speed differences between turbine and compressor may exist which then necessitate the addition of a gearbox or other workaround solution. Matching the SOFC exhaust gas flow to the maximum LPT flow capacity was considered to be the best approach as it avoided the need to vent compressor air flow to the surroundings, while the off-design flow delivered to the LP compressor still enabled a high-efficiency operating point to be achieved.

A high-level engineering design change analysis was carried out by P&W to assess both the number and magnitude of changes required to modify an FT8-3 generator for integration with a pressurized IG-SOFC power plant. Removal of the high-pressure spool necessitates consideration of lubrication systems, secondary air systems management (bleed streams), exhaust and inlet volute designs, engine rotor dynamics, and engine gearbox/startup modifications. Overall, changes to the existing FT8-3 engine design are considered to be significantly simpler and more cost-effective than either making design changes to a different product line or in beginning a new turbine development program. Additionally, FT8 design changes are estimated to result in a 40% reduction in capital cost on the engine itself and a 10–15% overall capital cost reduction of the gas generator when considering the supporting hardware, sub-system, and parts count reduction. Other synergies, such as a reduction in turbine maintenance and an increase in engine life, are also anticipated due to the design changes outlined above.

3.4 Organic Rankine Cycle. The ORC technology to be integrated at the utility-scale is based on modular designs that do not have a strong pressure-flow coupling with the topping systems (i.e., syngas production, SOFC, and GT) due to thermal integration via indirect transfer heat exchangers. ORCs are similar to steam Rankine cycle systems in that they consist of turbine, condenser (air-cooled or water-cooled), pump, and evaporator components, yet they differ in the type of working fluid employed, which is usually an organic fluid such as a refrigerant whose specific type depends on the temperature of the heat source. The selection of an ORC system (versus a steam power cycle) is generally driven by the better match of power capacity and turbine design with low-temperature heat sources. While ORC power systems demonstrate lower efficiency than steam cycles, they may offer economic benefits that offset their performance disadvantage. ORC systems are typically modular, closed systems with flanged connections. The economic merit of an ORC power system is primarily associated with its comparatively lower installation and operating costs than the more conventional steam Rankine cycle system. Lower operating costs for ORCs are in part due to the packaged nature of the system, their capability for remote unattended operation, and the lack of water treatment systems typically required for steam Rankine cycles. Ultimately, a detailed plant economic analysis is required to properly assess the net benefits of ORC technology at this scale, but such an effort is outside the scope of this work. Importantly, one aspect of this study is to simply quantify the performance potential of ORC integrated IGFC systems and compare them with a more conventional steam Rankine cycle configuration.

ORC technology can be scaled in capacity to match the waste heat exhaust from the SOFC and SOFC-GT subsystems. Two ORC technologies are examined in this study: (1) a scaled-up version of the 200 kW water-cooled, UTC PureCycle™ ORC product line and (2) the P&W Turboden HRS (high-electric efficiency units) product. PureCycle power scale-up is based on both increasing the size ($>10\times$) of an individual unit and combining units in parallel. The PureCycle system achieves a thermal efficiency of 14% from lower-temperature ($<150\,^{\circ}C$) heat sources and is based on an off-the-shelf Carrier compressor and the Carrier 19XR5 chiller. The turbine is combined with a high speed permanent magnet (PM) or traditional synchronous generator to convert the mechanical energy into electric energy. A high speed PM generator requires an ac/ac power electronic converter to connect to the 60 Hz electric grid. Heat rejection is accomplished with a cooling tower fed by the circulating water system. The efficiency of the water-cooled ORC system can be improved to 20%-LHV with a system design currently being targeted for development at UTC. The extent of the development for such a system to be integrated within the current IG-SOFC power plant concept requires heat exchanger redesign, optimal refrigerant selection, and expander impeller changes. In comparison, the Turboden HRS system can operate from heat sources as high as $500\,^{\circ}C$ and achieves net electric efficiencies exceeding 23% (LHV) for commercial systems in the 2.2 MW power range [21]. Power modules from Turboden are available up to 7 MW, thus three modules are envisioned for the present study. Both P&W PureCycle and Turboden systems are included the analysis, although the efficiency advantage of the Turboden is clear.

4 Modeling Approach

The component modeling effort draws upon the large library of fuel cell and combined heat and power (CHP) proprietary models developed by the United Technologies Research Center (UTRC) and its sister division, UTC Power. This library has been developed using the commercially available general process modelling system (gPROMS) software. The gPROMS software is an equation-oriented modeling system typically used within the process industry for building, validating, and executing first-principle models within a flowsheeting framework [22]. The software employs user-specified ODE and DAE simultaneous equation solvers to enable process modeling, simulation, parameter estimation, and optimization. It can be employed for either dynamic or steady-state modeling efforts. Steady-state modeling and simulation has been performed in this study.

4.1 Gasifier and Syngas Cleanup. Gasifier and syngas cleanup are not explicitly modeled but simply serve as boundary conditions to the system study. Gasifier and cleanup efficiency are assumed to be 82% from coal feed inlet to clean syngas outlet (see Fig. 5). Syngas composition entering the power block is approximated as 61% CO, 33.7% H_2, 2% CO_2, 0.3% H_2O, 2.0% N_2, and 1% Ar on a molar basis with sub-ppmv levels of H_2S, COS, mercury, ammonia, and chlorides. This composition is consistent with Shell gasifier technology operating near $1375\,^{\circ}C$ and 40 bar with molar feed ratios such that $O/C + H_2O/C \approx 1.1$ [10,20]. The oxy-combustor requires a pure O_2 stream that is supplied by the ASU at a marginal electrical energy cost of 0.285 kWh/kg O_2 as estimated from the literature [23–26].

Catalytic gasification technology is the focus of several DOE-sponsored IGFC studies (e.g., Ref. [18]) as it can generate methane molar concentrations as high as 20% in the syngas which provides enhanced thermal management for the SOFC stack due to internal reforming. However, given the sparse performance and operating information for catalytic gasification, the more proven Shell gasifier technology was selected for these integration studies.

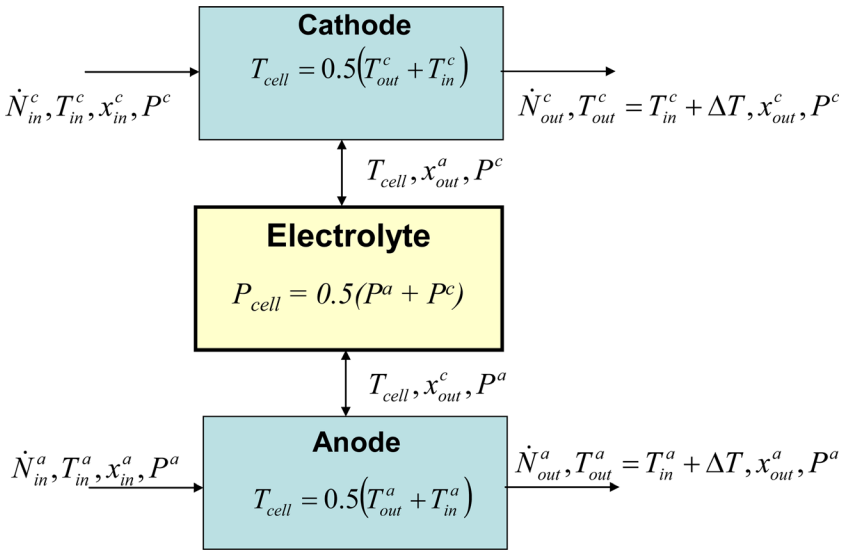

Fig. 3 SOFC stack model overview

4.2 SOFC System Modeling. The SOFC stack model is based on a lumped, single-node thermodynamic representation that accounts for internal reforming and water-gas shift equilibrium, electrochemical polarizations and the associated heat generation, mass transfer via cell reactions, and overall energy balances within a single-cell repeat unit. Reactant gas supply is assumed to be uniformly distributed among the cells within the cell-stack and among the channels within each repeat unit. Thus, single-cell performance is extrapolated to produce SOFC stack performance. This representation can be readily constructed as quantities such as stack voltage and stack power are scaled versions of single-cell voltage and power. Thus, a single-cell model forms the heart of stack system model. A coflow reactant gas configuration is envisioned for the SOFC stack as little to no methane is present in the coal syngas and thus, internal reforming is not active with the anode compartment.

Figure 3 depicts the architecture of a single-cell model where the ΔT across the cathode is typically specified, and T_{cell} and P_{cell} are the temperature and pressure at which all of the electrochemistry functions are evaluated. The model is comprised of three compartments – the anode, the cathode, and the electrolyte. Mass balances are written individually for the anode and the cathode compartments taking into account that the consumption of H_2 in the anode and O_2 in the cathode is governed by Faraday's law and is proportional to the current density. As given in the figure, $\dot{N}_i$ is the molar flow of species i, x_i is the molar fraction of species i, T is temperature, ΔT is temperature rise, and superscripts "a" and "c" refer to anode and cathode compartments, respectively. It is assumed that hydrocarbons and carbon monoxide are not electrochemically active but are consumed rather through reforming and water-gas shift (WGS) reactions. For coal syngases, H_2 and CO dominate the anode feed gas composition and thus, the CO is shifted via WGS reactions to CO_2 and the produced H_2 then is the only participant in electrochemical oxidation at the triple-phase boundary. It is assumed that the WGS and reforming reactions are at equilibrium in the anode. Provision is made in the mass balance equations to account for compounds consumed/produced due to the WGS, reforming, and electrochemical reactions. Quantities such as fuel utilization and O_2-stoichiometry are calculated from the mass-balance equation framework.

An overall system energy balance is implemented as a part of the model. The total enthalpy-flow into the system has two components: the anode inlet flow and the cathode inlet flow. Similarly, the enthalpy-flow out of the system has the anode outlet and cathode outlet flow components. The lumped system produces power and rejects thermal energy to both the surroundings and the cathode cooling air stream.

The electrochemistry equations that describe the electrolyte compartment in the model are shown below:

$$V_{\text{ref}} = -\frac{\Delta G}{2F} + \frac{RT_{\text{cell}}}{2F}\ln\left(\frac{P_{\text{H}_2}}{P_{\text{H}_2\text{O}}}\sqrt{P_{\text{O}_2}(\text{bar})}\right) \tag{1}$$

$$R_{\text{ohm}} = \frac{L_E T_{\text{cell}}}{A_{\text{ohm}}}\exp\left(\frac{E_{\text{act-ohm}}}{RT_{\text{cell}}}\right) \tag{2}$$

$$V_{\text{act}} = \frac{RT}{2F}\sinh^{-1}\left(\frac{J}{A_{\text{act}}}\exp\left(\frac{E_{\text{act}}}{RT_{\text{cell}}}\right)\right) \tag{3}$$

$$V = V_{\text{ref}} - R_{\text{ohm}}J - V_{\text{act}} \tag{4}$$

where, V_{ref} is the open circuit voltage, R_{ohm} is the ohmic resistance (primarily due to electrolyte), L_E is the electrolyte thickness, V_{act} represents the activation losses, V is the cell voltage, J is the current density, T_{cell} is the temperature of the cell, and P_{H_2}, $P_{\text{H}_2\text{O}}$, and P_{O_2} are the partial pressures of hydrogen, water, and oxygen, respectively, taken at the tail-gas outlet. All other quantities in Eqs. (1)–(4) are model parameters that were initially tuned to be representative of near-term anode-supported planar SOFC technology [27]. These other model parameters include A_{act}, a charge transfer coefficient parameter and activation energies ($E_{\text{act-ohm}}$ and E_{act}). Cell power density was increased by V-I slope adjustment to obtain performance that was consistent with SECA targets of 0.45 W/cm^2 on syngas. Concentration polarization is neglected in this model as (i) the electrochemical model with the parameters given above provided sufficient fidelity to reproduce V-I curves from developers data and (ii) the voltage-current response is dominated by the transfer of electrons through the cell trilayer and across the material interfaces at low- and mid-range current densities of anode-supported SOFCs [28]. The cell operating conditions in the following analyses are far away from the high current region that is dominated by diffusion limitations in the porous anode. The resulting model-generated single-cell V-j (voltage-current density) curve is depicted in Fig. 4.

4.3 Gas Turbine Modeling. An integral part of the system component models are the performance maps for the P&W FT8-3 gas turbine. Conventional turbine and compressor performance maps typically involve speed as one of the inputs, and the outputs

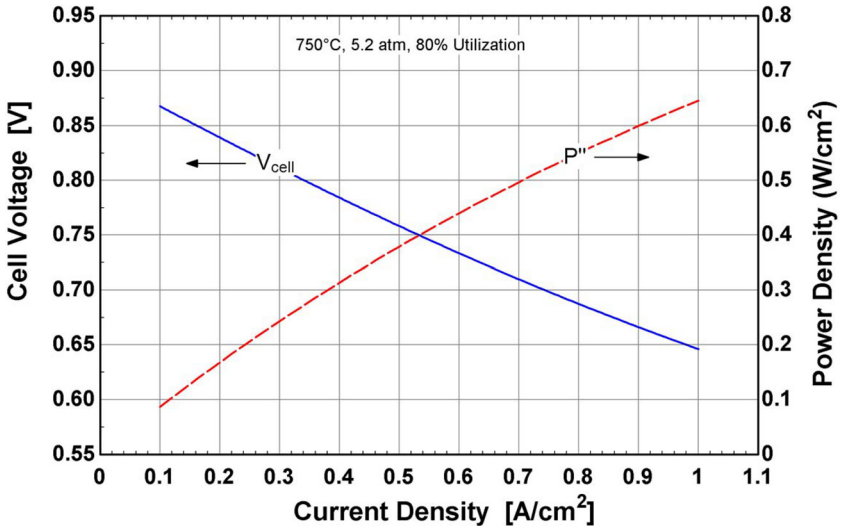

Fig. 4 SOFC V-j model performance characteristic

include quantities such as pressure ratio and efficiency. As speed is more of a design variable and is not of interest as far as system studies are concerned, the functional input/output format of the performance map was reversed. The LPC inputs consist of the mass flow through a compressor, and the pressure ratio (PR) associated with the compressor. The conditions for the inlet air are fixed at 15 °C and 1 atm pressure. Given these two inputs, the performance maps predict the compressor efficiency from which quantities, such as power required for compression and compressor outlet temperature can be obtained using simple thermodynamic calculations. Based on tests with residuals obtained using different polynomial functions, the following functional form was deemed most suitable:

$$\eta_{\mathrm{LPC}} = \sum_{i=0}^{2}\sum_{j=0}^{2} a_{a_{i+j}} (\mathrm{PR})^i (\mathrm{Mass\ Flow})^j \tag{5}$$

The advantage of the above functional form is that the process of obtaining the polynomial coefficients can be cast as a linear-least-squares optimization problem, which is easily solved using MS-Excel's SOLVER tool.

In the case of the LPT, the operational speed can be adjusted so as to maintain a constant efficiency of 91.8%, but at the cost of altering the expansion pressure ratio (PR) with different inlet conditions. Thus, the expansion pressure ratio of the LPT is defined as a function of the inlet temperature. If the inlet stream conditions (mass flow, temperature and pressure) are specified, then efficiency and pressure ratio can be calculated, which in turn can be used to calculate the outlet stream properties and the power obtained from the expansion process. In the case of the power turbine (PT), the outlet pressure is fixed at 1.016 atm and the inlet pressure is determined by the outlet pressure of the LPT. The PT efficiency is observed to be a function of inlet temperature (in K) and pressure (in atm). The functional form for the efficiency curve is given by

$$\eta_{PT} = \left(\sum_{i=0}^{4} a_i P_{\mathrm{in}}^i\right)\left(\sum_{i=0}^{3} b_i \left(\frac{T_{\mathrm{in}}}{1000}\right)^i\right) \tag{6}$$

The above functional form was chosen after several trials with different functional forms. The optimization problem in this case is a nonlinear-least squares problem, which was also solved using MS-Excel's SOLVER tool. Given the inlet pressure and temperature the performance map predicts the PT efficiency from which quantities such as power obtained from the expansion process and PT outlet temperature can be obtained using simple thermodynamic calculations.

4.4 Bottoming Rankine Cycle (ORC or SRC) Modeling. The work in this paper does not explicitly model ORC and steam turbine systems, but assumes that the available thermal energy from various process streams in the plant can be used to produce power at a specified thermal efficiency. Performance modeling of the ORC system is derived from the UTC PureCycle water-cooled product line which at the 200 kW-scale achieves a thermal efficiency of 14%. When scaling up to 20 MW, and employing a higher source temperature for heat addition to the cycle, changes to the PureCycle ORC system design are necessary. After a preliminary engineering analysis of such changes, it is estimated that a 20% efficiency performance is achievable with a redesign of the PureCycle system that moves to higher system temperatures and pressures in conjunction with changes to the generator speed and approaches to the associated bearing and gear lubrication. A higher temperature ORC system was also examined via the Pratt & Whitney TurboDen ORC product line. Net efficiency performance for heat recovery from turbine exhaust ranges from 23.3 to 23.6% [29]. Finally, to facilitate a comparison between ORC and SRC systems, a 30-MW class steam turbine cycle is evaluated using an estimated net thermal efficiency of 31% based on several literature references [16,30,31]. A simple model that sums all heat additions and employs an overall thermal efficiency is used to estimate power production according to the relation $\dot{W}_{\mathrm{ORC}} = \eta_{\mathrm{ORC}} \sum_j \dot{Q}_{\mathrm{in},j}$.

4.5 Definition of Performance Metrics. System performance metrics used throughout the subsequent sections of the systems analysis are defined in the following equations. Efficiency bases with and without CO_2 capture and sequestration are also provided:

$$\eta_{\mathrm{coal}} = \frac{\dot{W}_{\mathrm{sys,net}}}{\dot{m}_{\mathrm{coal}} \cdot LHV_{\mathrm{coal}}} = \eta_{\mathrm{syngas}} \cdot \eta_{\mathrm{gasifier}} \tag{7}$$

$$\eta_{\mathrm{gasifier}} = \frac{\dot{m}_{\mathrm{syngas}} \cdot LHV_{\mathrm{syngas}}}{\dot{m}_{\mathrm{coal}} LHV_{\mathrm{coal}}} \tag{8}$$

$$\eta_{\mathrm{syngas}} = \frac{\dot{W}_{\mathrm{sys,net}}}{\dot{m}_{\mathrm{syngas}} \cdot LHV_{\mathrm{syngas}}} \tag{9}$$

$$\eta_{\mathrm{coal,CO_2}} = \frac{\dot{W}_{\mathrm{sys,net}}}{\dot{m}_{\mathrm{coal}} \cdot LHV_{\mathrm{coal}} + \dot{E}_{\mathrm{sep}} + \dot{W}_{\mathrm{CO_2}}} \tag{10}$$

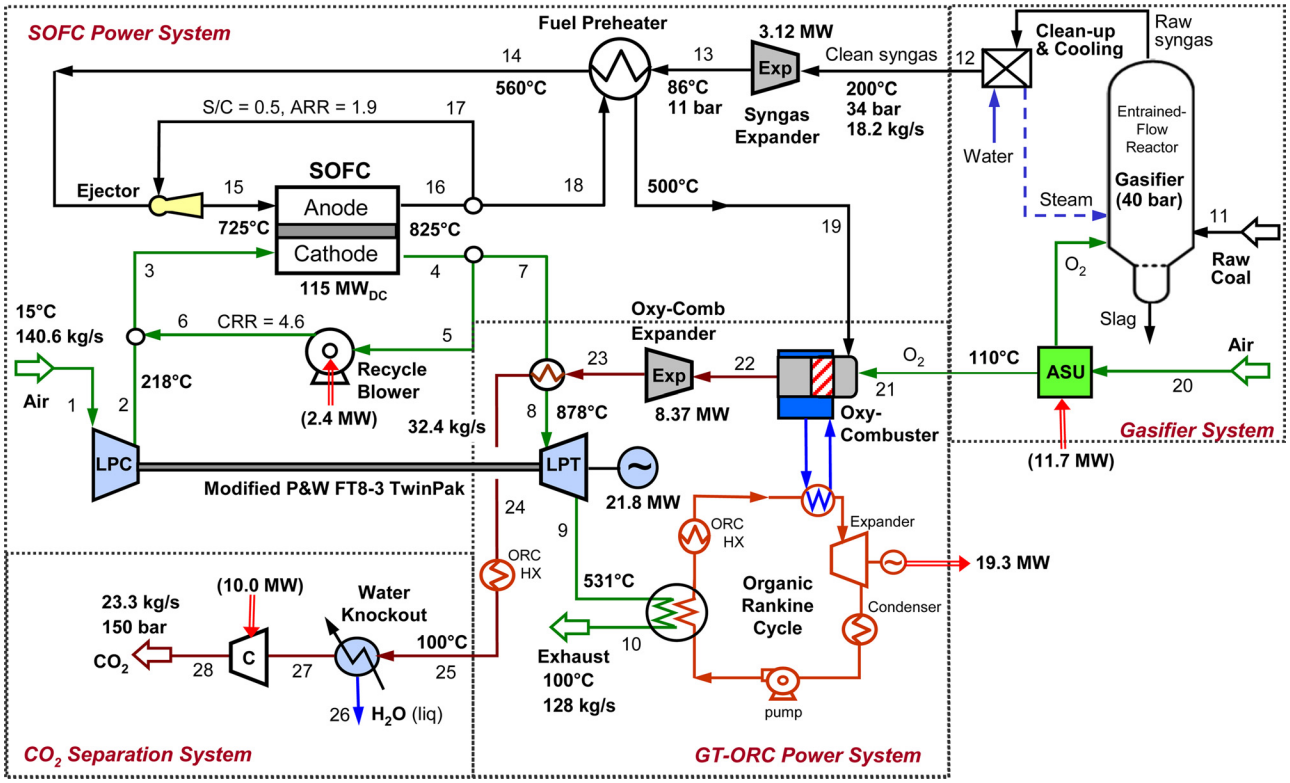

Fig. 5 Hybrid IGFC plant concept flowsheet depicting gasifier, SOFC, GT-ORC, and CC&S subsystems

$$\eta_{\mathrm{ORC}} = \frac{\dot{W}_{\mathrm{ORC}}}{\dot{Q}_{\mathrm{ORC,in}}} \tag{11}$$

$$\dot{W}_{\mathrm{sys,net}} = \dot{W}_{\mathrm{SOFC}} + \dot{W}_{\mathrm{FT8,net}} + \dot{W}_{\mathrm{ORC}} + \sum_i \dot{W}_{\mathrm{exp},i} - \dot{W}_{\mathrm{blower}} - \dot{W}_{\mathrm{CO_2}} - \dot{E}_{\mathrm{sep}} - \dot{E}_{\mathrm{ASU}} \tag{12}$$

where $\dot{W}_{\mathrm{sys,net}}$ is the net ac electric power derived from the IGFC power plant including SOFC ($\dot{W}_{\mathrm{SOFC}}$), gas turbine ($\dot{W}_{\mathrm{FT8,net}}$), syngas expanders ($\dot{W}_{\mathrm{exp}}$), and ORC power subsystems ($\dot{W}_{\mathrm{ORC}}$). $\dot{E}_{\mathrm{sep}}$ is the energy spent in supplying cooling water for water knockout and regeneration of water sorbents, $\dot{W}_{\mathrm{CO_2}}$ is the compression work required to raise the captured CO_2 to pipeline sequestration-ready conditions (150 bar). $\dot{W}_{\mathrm{blower}}$ is the power required by the cathode recycle blower. $\dot{E}_{\mathrm{ASU}}$ is the electric power required to operate the air separation unit. $\dot{Q}_{\mathrm{ORC,in}}$ is the net thermal energy addition to the ORC system. LHV_{syngas} is the lower heating value of the gasifier syngas downstream of gas cleanup and cooling.

5 IGFC System Concept Design and Analysis

Initial studies of IGFC plant concepts established the DC power rating of the SOFC power block near 115 MW and focused on integrating the SOFC power section with the P&W FT8 gas turbine and a scaled-up version of the PureCycle organic rankine cycle waste heat power generator. The resulting system concept is presented in Fig. 5. A pure oxygen stream is supplied from the gasifier air-separation plant to the oxycombustor which oxidizes the anode tail-gas, thereby producing only CO_2, H_2O, and a small amount of N_2. The anode tail-gas is not mixed with the cathode exhaust gas stream and thereby, makes the process for CO_2 separation and capture a simple one through the use of a condenser to knock-out the water vapor present in the stream. The system also employs hot cathode gas recycle. The power plant concept is projected to have a capacity of 149 MW at 51.4%-LHV (48.1%-HHV) efficiency without CO_2 capture and compression costs and 139 MW at ~48%-LHV efficiency with CO_2 capture to sequestration-ready pipeline conditions [32].

The incoming system air at station (1) is compressed to the system pressure ratio of 5.2 using the LPC from the modified P&W FT8 engine. The LPC has a well-defined performance map where the efficiency is a function of the mass flow rate of air through the system and the compressor PR. The conditions (flow, temperature and pressure) of stream (2) are such that when mixed with the cathode recirculation stream (6), the conditions of the resulting stream (3) meet the inlet requirements of the cathode compartment of the SOFC stack. Part of the stack cathode exhaust stream is re-circulated (5) with a high-temperature cathode recycle blower. The balance of the flow (7) receives thermal energy transferred from the oxygen burner outlet stream. Burner product gases transfer heat to the cathode exhaust in a high-temperature heat exchanger. The constraint on the heat-exchanger is that it should maintain a pinch temperature of at least 15 °C and at the same time ensure that the outlet temperature of stream (8) is as close to 950 °C, which is the maximum allowable LPT inlet temperature. The modified FT8 TwinPak requires a flow split for the two sets of parallel turbines (not shown). As described previously, each turbine set is comprised of a low-pressure turbine whose expansion pressure ratio is on the order of 2.5, a power turbine whose outlet pressure is close to atmospheric pressure (~1.01 bar), and synchronous 60 Hz electric generator. The thermal energy accompanying the turbine exhaust gases (9) is transferred to the bottoming ORC heat engine via a heat recovery refrigerant economizer/evaporator before being vented out as exhaust gas at a temperature of 100 °C (10).

Raw coal is fed to the entrained-flow gasifier plant where it is mixed with oxygen at a molar O_2/C ratio of 0.48 and steam at an H_2O/C ratio of 0.10. The composition of the H_2/CO-rich syngas exiting the gasifier is generated using equilibrium at the gasifier operating temperature of 1375 °C and 40 bar. After quench cooling, scrubbing, and cleanup, the high-pressure syngas (34 bar) is expanded in a turbine generating over 3 MW of power. The expander outlet gas (13) is supplied to the SOFC power block at

Table 2 Performance summary for hybrid IGFC system

	Bottoming Cycle Type		
	PureCycle ORC	TurboDen ORC	SRC
Fuel In			
Raw Coal, MW (LHV)	290	290	290
Syngas,[a] MW (LHV)	238	238	238
Power (MW)			
SOFC, MW_{AC}	111		
GT	21.8		
Rankine Bottoming Cycle (ORC or SRC)	19.3	22.7	29.9
Oxycombustor Expander	8.37		
SynGas Expander	3.08		
ASU O_2 and N_2 supply	−11.9		
CO_2 compression	−10.0		
Absorbent regen. and misc. CC&S power	−0.5		
Recycle Blower	−2.4		
Net Power on syngas	156.3	159.7	167.0
Net Power on syngas with CC&S	145.8	149.2	156.5
Net Power on coal	149.3	152.6	159.9
Net Power on coal with CC&S	138.8	142.1	149.4
Efficiencies (%)			
Gasifier	82.0		
Recycle blower	50.0		
Dc/Ac Inverter	96.5		
Expanders	88.0		
FT-8 LPC	84.0		
FT-8 LPT	91.8		
FT-8 PT	85.8		
ORC or SRC (net)	20.0	23.5	31.0
CO_2 Compression	82.0		
System Performance (%-LHV)			
Net Efficiency on syngas	65.7	67.1	70.2
Net Efficiency on syngas with CC&S	61.3	62.7	65.7
Net Efficiency on coal	51.5	52.6	55.1
Net Efficiency on coal with CC&S	47.8	49.0	51.5

[a]Syngas refers to the coal gasifier outlet and is not a plant input.

elevated pressure (∼11 bar) and temperature (60 °C). In the fuel preheater, the fuel-gas is preheated to a temperature (14) such that, when mixed with the re-circulated anode exhaust stream (17), its temperature matches the temperature and pressure of the stack anode inlet (15) while maintaining a steam-to-carbon ratio of 0.5 to minimize the potential carbon deposition and soot formation within the stack manifolding and anode gas channels. With this level of recycle, the resulting oxygen-to-carbon and hydrogen-to-carbon ratios of the anode inlet gas are well-below the threshold for carbon formation at 725 °C based on calculations for C–H–O equilibrium using ternery diagrams (cf. Refs. [16,33]). It is further envisioned that piping for the anode feed gas will be made from zinc-free, copper-lined alloys or alumina-coated stainless steels to essentially eliminate catalytically activated (carbon forming) nucleation sites on piping inner surfaces. The syngas supply pressure is sufficiently high to drive the gas ejector to provide the anode exhaust gas recycle flow. The supply pressure to the gas ejector has been conservatively estimated by simulation of a gas ejector operating with an ejector efficiency[3] of 20% as well as confirmation checks with Ref. [34]. The required gas ejector supply pressure then establishes the minimum outlet pressure of the syngas expander. While a portion of the anode tail-gas is re-circulated, the thermal energy accompanying the balance of the flow (18) is used to preheat the coal syngas in the fuel preheater. The residual fuel in the anode tail-gas stream is then burned in the oxygen combustor using O_2 supplied by the "oversized" ASU.

In order to ensure complete combustion in the oxycombustor, excess oxygen is supplied such that there is a molar concentration of 0.1% O_2 in the product gas. This relatively low value of excess oxygen has been selected in part to meet DOE guidelines for non-condensables in CO_2 sequestration pipelines and to minimize ASU parasitic power. In contrast, some studies supply excess oxygen such that a concentration of 1% O_2 is obtained in the combustion products [18]. While the low value of excess oxygen required is optimistic, the impact of this value (in the range of 0.1 to 1%) on overall plant efficiency is negligible (less than 0.1%). The use of pure oxygen in the combustor can generate gas temperatures higher than 1500 °C depending on the amount of fuel utilization and presents material and durability issues in combustor design. The present concept is to employ an actively-cooled burner tube which would limit combustor temperatures to 1100 °C. Heat rejection from the burner tube would then be transferred to the ORC unit in a separate heat exchanger. (Another alternative is to recycle cooler oxy-combustion product gases back to the burner inlet using a gas ejector driven by the anode tail-gas.) The oxy-combustor combustion gases are then expanded down to 2 bar, producing nearly 8.4 MW of additional power. The inlet gas temperature of the LPT can be as high as 950 °C. To take advantage of this capability, a regenerative heat exchanger is shown in Fig. 5 to boost the cathode tail-gas temperature from 825 °C to almost 880 °C with the goal of making it as close to 950 °C as possible. This heat exchanger has severe temperature requirements and is envisioned to be a rotating, ceramic core regenerative-type heat exchanger currently being developed for 300 kW microturbines in

[3]Ejector efficiency is defined as $\eta_{\text{ejector}} = \frac{\dot{V}_2 P_2 \ln(P_3/P_2)}{\dot{V}_1 (P_1 - P_3)}$, where $\dot{V}$ is the volumetric flow rate and P is the static pressure at the denoted location in the ejector. The subscripts 1, 2, and 3 refer to the primary driving flow (fresh air), the secondary flow (recycle), and the mixed flow at the ejector outlet, respectively.

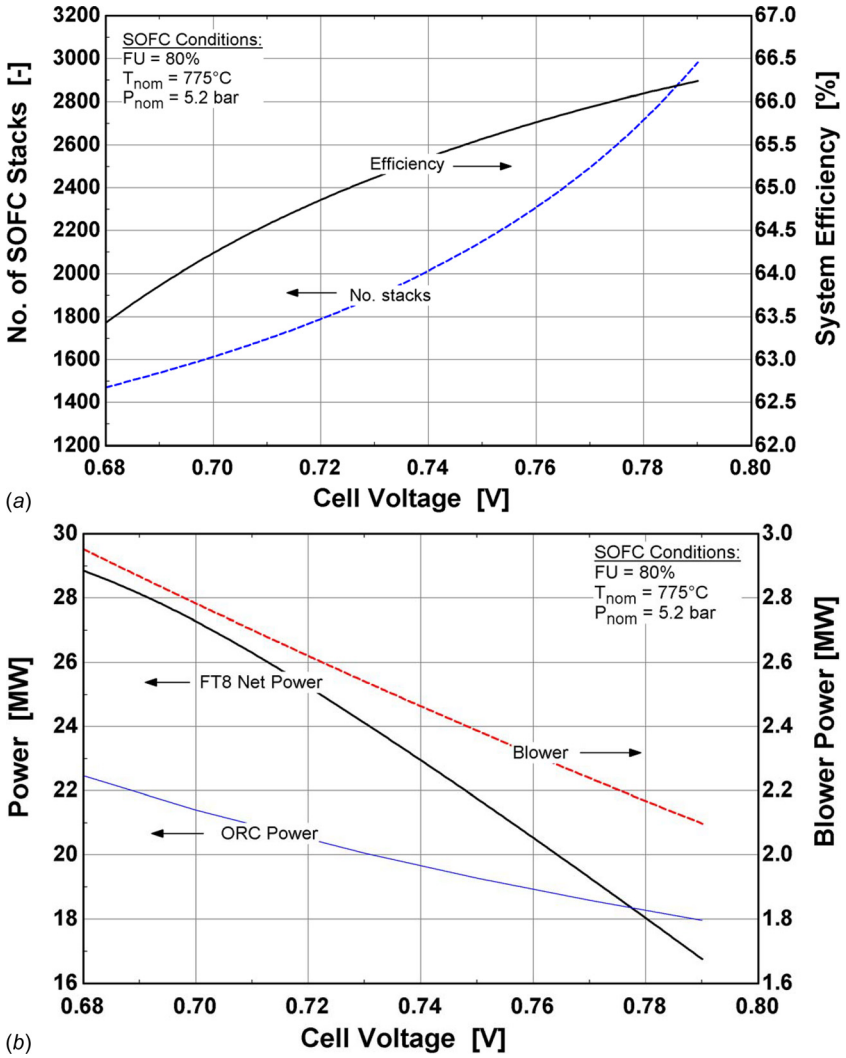

Fig. 6 Effect of cell voltage on system parameters associated with the hybrid IGFC system

distributed generation applications [35]. Finally, the remaining thermal energy associated with the burner outlet stream at station (22) is transferred to the ORC in a lower-temperature heat exchanger (750–800 °C) made from high-grade stainless steel or a high-temperature alloy. This oxygen combustor product gas stream contains mostly CO_2 and H_2O. After condensing out the water with a combination of cooling and a conventional water absorbent (e.g., triethylene glycol mixture or lithium-chloride solution), 90% of the CO_2 is compressed to 150 bar (2200 psig) and piped to a sequestration location (28), with the remaining 10% vented to the atmosphere. Thus, the ORC has three primary heat addition sources: (i) thermal energy transfer from the water-cooled oxygen combustor tube, (ii) the hot exhaust gas from the power turbine, and (iii) the high-temperature heat exchanger located between stations (23) and (24). The arrangement of heat exchangers shown in the ORC of Fig. 5 is not intended to be representative of an actual heat exchanger network integration scheme.

Table 2 summarizes the hybrid system performance including the overall impact to the system when accounting for the energy requirements of carbon capture and storage. CCS in this paper includes CO_2 separation via water knockout and a conventional water absorbent, and CO_2 compression to pipeline sequestration conditions of 150 bar [32]. Energy requirements for regeneration of the water sorbent and pumping of the coolant flow for the water knockout heat exchanger are unknown, but assumed to be 5% of the CO_2 compression power for the purposes of this study. The power plant generates 156 MW of net ac power, where the redesigned FT8 and the scaled-up UTC Power PureCycle sub-systems contributing nearly 20 MW each. The SOFC operates nominally at 775 °C with an average cell voltage of 0.75 V, a fuel utilization of 80%, a power density of 0.45 W/cm^2, a 100 °C temperature rise across both the anode and the cathode, and a 2.5 kPa pressure drop across the cathode. The SOFC power block provides about 68% of the total gross power from the plant, the gas turbine and scaled-up ORC systems supply approximately 13 and 12%, respectively, and the gas expanders about 7%. The compression of CO_2 using intercooled compression stages each at 82% isentropic efficiency [24] to sequestration-ready pressure levels requires about 10 MW of power. The LPC, LPT, and PT operate at 84.0, 91.8, and 85.8% isentropic efficiencies, respectively. The recycle blower operates at 50% efficiency (52.6% isentropic) and consumes about 2.4 MW of power for a cathode recycle ratio of 4.6 and a cathode recycle loop pressure rise requirement of 3 kPa. Efficiencies reported in Table 2 are total efficiencies, that is, they include motor and mechanical inefficiencies. Thus, in the case of the FT8 turbines and CO_2 compressor, the mechanical efficiency is approximated to nearly 100%.

The net system efficiency of the power plant employing the modified PureCycle ORC bottoming cycle is 65.7% (LHV) when operating from clean syngas supplied at the fuel preheater inlet, and 51.5% on raw coal (i.e., accounting for the inefficiency in the gasifier). Syngas-based system performance includes the power

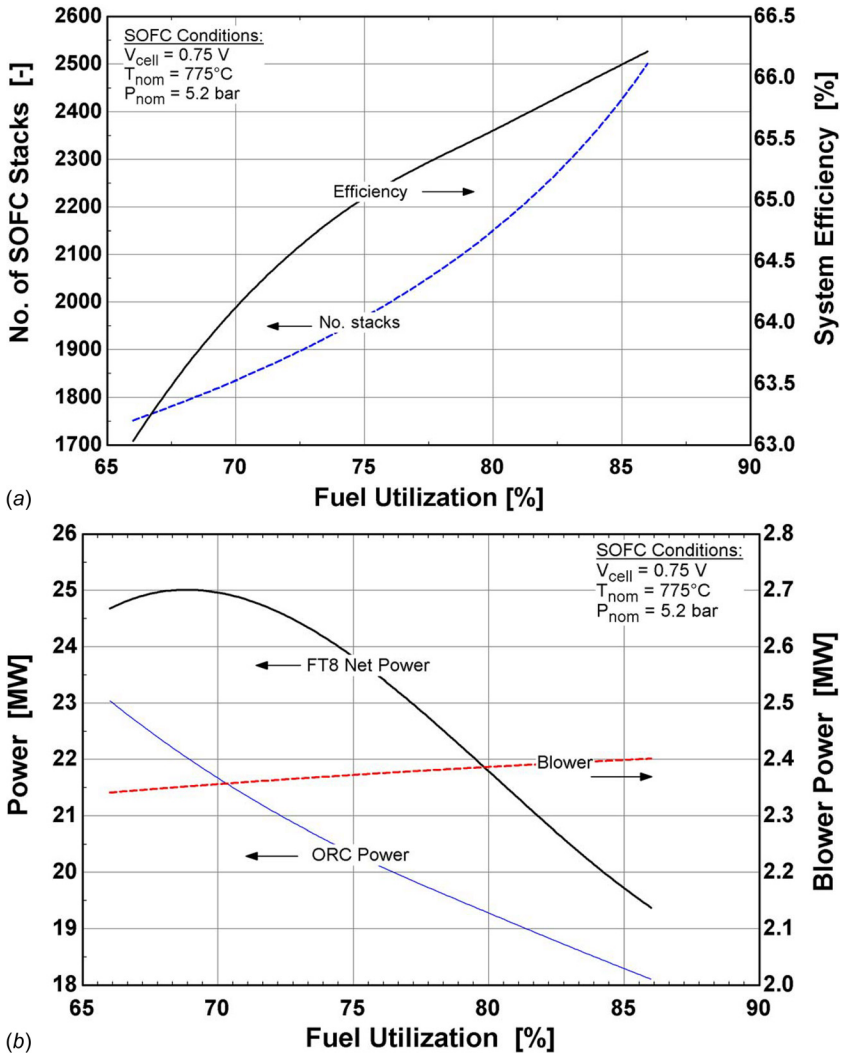

Fig. 7 Effect of fuel utilization on system parameters associated with the hybrid IGFC system

generated from the oxycombustor expander, but not the syngas expander, and includes the power required to supply O_2 to the oxycombustor (1.7 MW). The total system performance after including the energy requirements for CCS reduces the net system efficiency to 61.3 and 47.8% when based on clean syngas and raw coal feedstocks, respectively. The use of the P&W ORC Turbo-Den product line offers a bottoming cycle efficiency improvement of 3.5% and increases the net efficiency of the system on syngas to 67.1% and to 49.0% on coal with CCS. These IGFC plants using ORC bottoming cycles with CCS amount to 14.0 and 15.2 percentage point improvements in efficiency, respectively, over conventional IGCC/CCS power plant performance (estimated at ~33.8%-LHV in Ref. [1].).

The high-grade thermal energy that is available for input into the ORC subsystem suggests that a steam-based rankine power subsystem is also viable. Indeed, while the purpose of this study was to investigate the performance with primarily ORC systems, a steam turbine plant potentially offers even higher efficiency depending on the boiler pressure and superheat temperatures achievable. Assuming a simple rankine cycle net efficiency of 31%, the IGFC system efficiency on coal could produce about 10.6 MW of additional power and increase net system efficiency by 3.7-percentage points to 55.1% (51.5% with CCS).

5.1 IGFC Parameter Sensitivity Study. Having established the baseline performance, select system parameters were varied and the sensitivity of these parameters to the baseline IGFC system was evaluated. Cell voltage, fuel utilization, system pressure ratio, anode S/C ratio, cathode-side pressure drop, and stack ΔT were the system parameters varied. The dc power from the stack was fixed at 115 MW throughout this study. Given a cell planform and a fixed number of cells per stack, the number of stacks is then calculated based on design voltage, and overall power setting. This provides an estimate of fuel cell power density. Figures 6–11 present trends in system performance metrics such as efficiency, number of stacks required, total power from the gas turbine system, power obtained from the PureCycle ORC unit, and recycle blower parasitic power as functions of the different parameters. Importantly, in order to separate out the gasifier efficiency considerations, the efficiency reported in the following analyses is the net system efficiency from syngas without CCS penalties.

Figure 6 illustrates the effect of cell voltage on system efficiency, power density (as reflected by the number of cell-stacks), and parasitic power in the system. An increase in voltage results in lower blower parasitic power, as well as, as a reduction in total power produced by the FT8 and PureCycle ORC systems. Reductions in power output from the bottoming cycles occur because increasing cell voltage translates into increasing cell-stack efficiency, and correspondingly lower quantities of waste heat in the product gas. It is interesting to observe that stack power density is nearly halved by an increase in cell voltage of only 100 mV. Such high sensitivity of power density to changes in cell voltage is

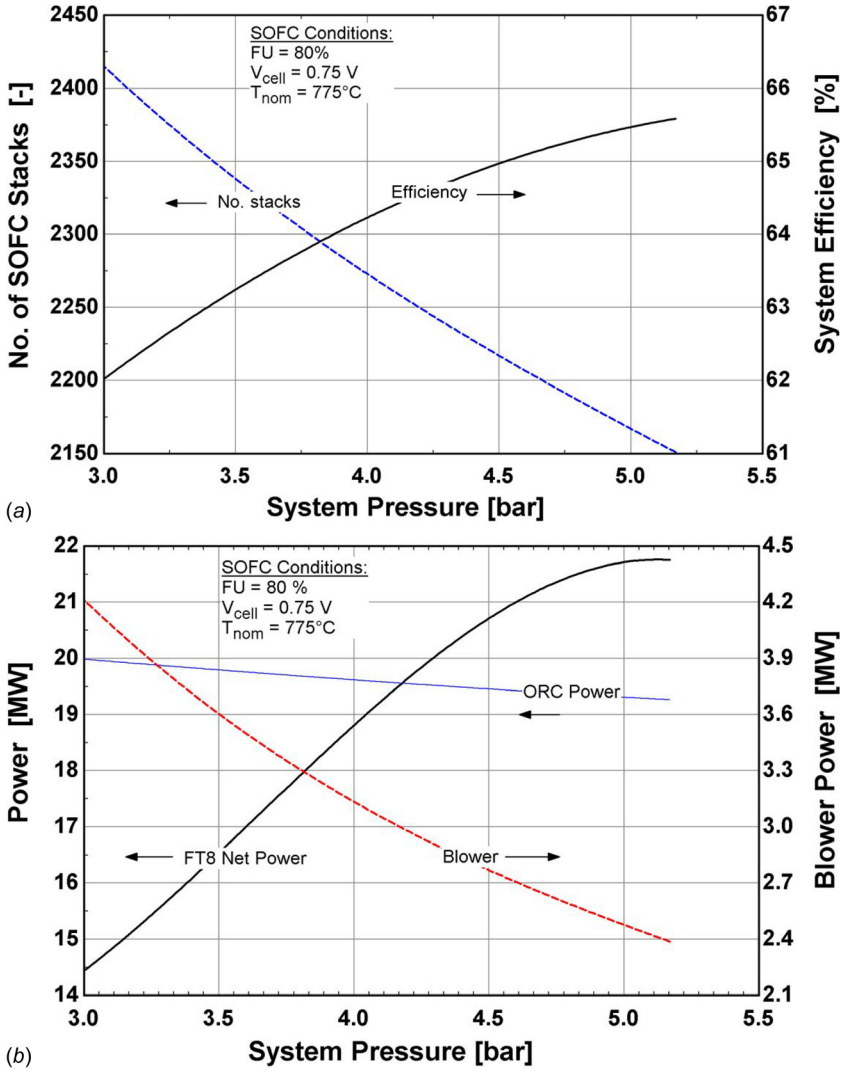

Fig. 8 Effect of system pressure ratio on system parameters associated with the hybrid IGFC system

explained by the cell V-j performance characteristic previously given in Fig. 4. For example, at 0.7 V, the single-cell power density is approximately 0.53 W/cm^2. At 0.8 V, the power density is about 0.27 W/cm^2. Thus, while high-performance, high power density cell-stacks can be cheaper and more efficient, the shallow slope of their V-j characteristic is such that small changes in voltage result in large changes in operating current.

The effect of fuel utilization on performance is shown in Fig. 7. At a prescribed cell voltage, system efficiency is correlated with fuel utilization as is ORC power production. The increase in net system efficiency is off-set by reductions in FT8 and ORC power production. The power density of the SOFC is also lowered with increasing fuel utilization as revealed in the figure by the increasing number of SOFC stacks required. Interestingly, net power from the FT8 gas turbine system reaches a maximum at a fuel utilization of 70%. Further increases in gas turbine power production with decreasing fuel utilization are constrained by turbine inlet temperature limits. Increases in SOFC fuel utilization lower the energy available in the tail-gas and thereby, lower the power output of the FT8. The bottoming ORC power output is directly correlated with fuel utilization and as expected, decreases with increasing fuel utilization due to lower available thermal energy associated with the burner outlet stream.

Operating the power plant system at elevated pressure is very important to achieving SOFC power density goals of 0.45 W/cm^2, as Fig. 8 shows. Net system efficiency also benefits substantially (~3.5 percentage points) when increasing the system pressure from 3 to 5.2 bar operation. The cathode recycle blower power parasitic decreases substantially (~43%) in response to increases in system operating pressure due to reductions in hot gas density and hence, volume flow rate. However, the primary factors that enable higher system efficiency from increasing the system pressure arise from higher efficiency SOFC and FT8 gas turbine operation. Higher efficiency SOFC operation in response to elevated pressure is well-documented (e.g., Ref. [36]). The FT8 produces some 57% more net power by design point allowing the LPT shaft power to increase incrementally more than the increase in the LPC power consumption.

The presence of carbon monoxide (CO) in the dry coal-gas stream delivered to the power plant requires consideration of coking formation side reactions within piping runs and hardware. In particular, as noted by Probstein and Hicks [33], fuel gas mixtures with O/C ratios of 1.0 and H/C ratios of 2 are likely to form carbon in the temperature range between 625–925 °C. The Boudouard coking mechanism can be inhibited and/or controlled with steam injection. The approach taken in the system design efforts to limit the potential for undesirable coke formation is centered on a two-pronged strategy where (1) fuel gas piping is lined with copper or oxide layers that minimize nucleation sites for coke formation and (2) injecting steam (albeit at a lower steam-to-carbon ratio) into the fuel syngas stream via an ejector and anode gas recycle. Since the coal fuel gas provided by the gasifier is

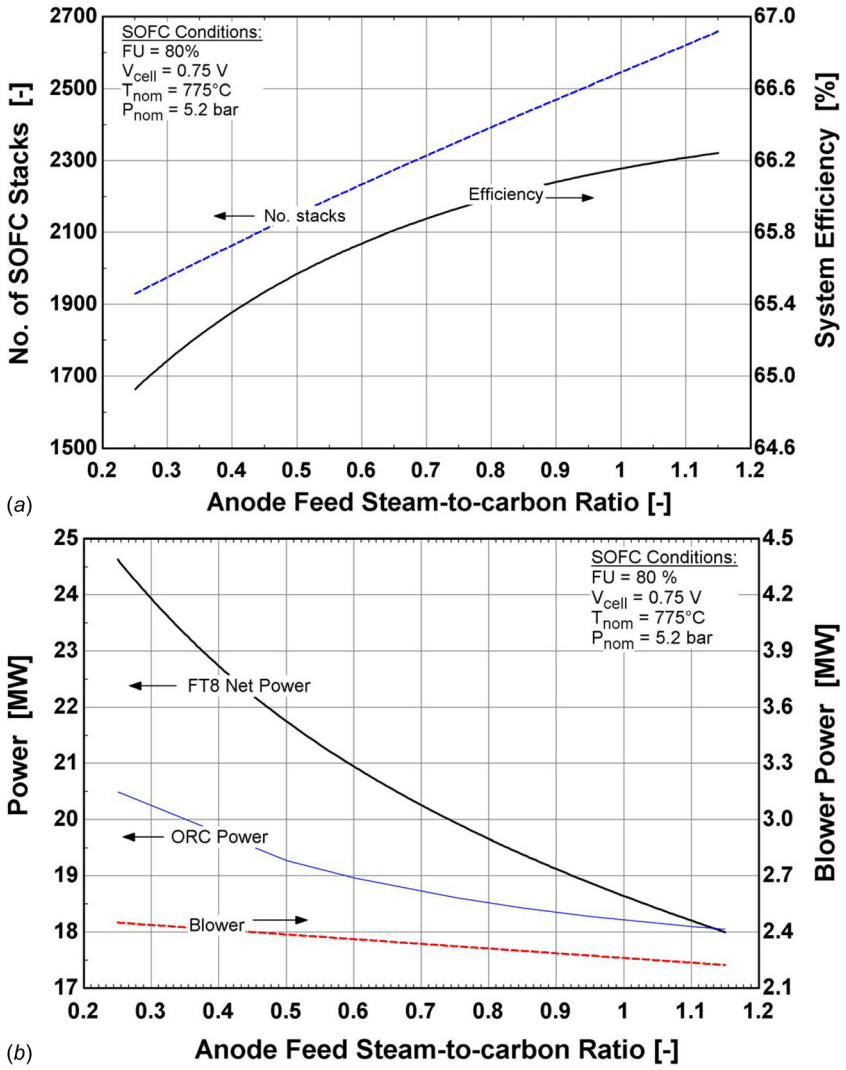

Fig. 9 Effect of anode S/C ratio on system parameters

significantly pressurized, the ejector can be effectively driven to provide the desired recycle flows.

Figure 9 relates the effect of steam-to-carbon (SC) ratio on system performance. Note again that as with the previous analyses, the design cell voltage has been fixed in this parameter variation. One of the main effects of increasing SC ratios is the reduction in SOFC power density due to dilution of the anode gas feed and hence, a lowering of the Nernst potential. This dramatically increases the number of fuel cell stacks required to deliver 115 MW of power. The overall system efficiency is also correlated with the amount of anode recycle (and hence, SC). Interestingly, the increase in SC ratio produces an increase in system efficiency even though the bottoming cycle power production is reduced. The root of this performance change is related to an increase in effective *system* fuel utilization. In this analysis, the per-pass (or in-cell) fuel utilization was held constant at 80%. The increase in recycle actually increases the overall *system* fuel utilization. Thus, the system efficiency trends with increasing SC are not unlike those of increasing per pass fuel utilization within the SOFC (although the concavity of the plots is different).

Figures 10 and 11 depict the sensitivity of cathode side pressure drop and temperature rise on system performance, respectively. While the recycle blower parasitic power appears to be strongly influenced by cathode loop pressure drop, it is actually a relatively mild effect when considering pressurized gas flows and the percentage of net power production from the plant. There is a much stronger system-level efficiency effect associated with cathode pressure drop in near-ambient pressure SOFC systems (i.e., 1.0 to 1.1 bar). Cathode temperature rise has a direct influence on SOFC power density due to increases in per pass oxidant utilization as Fig. 11 shows, but the system efficiency and net power production from the ORC are only mildly affected. The net FT8 power production is slightly decreased due to the reduction in mass flow through the unit. While cathode temperature rise can provide substantial blower parasitic power reductions, greater *system* efficiency advantages can be obtained with increases in cell temperature [37].

6 Summary

Overall, while efficiency is reasonably correlated to fuel utilization, system pressure and anode S/C ratio, the number of stacks required to achieve 115 MW from the SOFC system is sensitive to each of these parameters. An optimal selection of parameters is possible if cost data are available. This has not been attempted in the current study, and will be considered in future studies.

Given that the parametric analyses did not include the gasifier technology and performance, system integration advantages may be overlooked. In general, by fixing the SOFC stack power, the

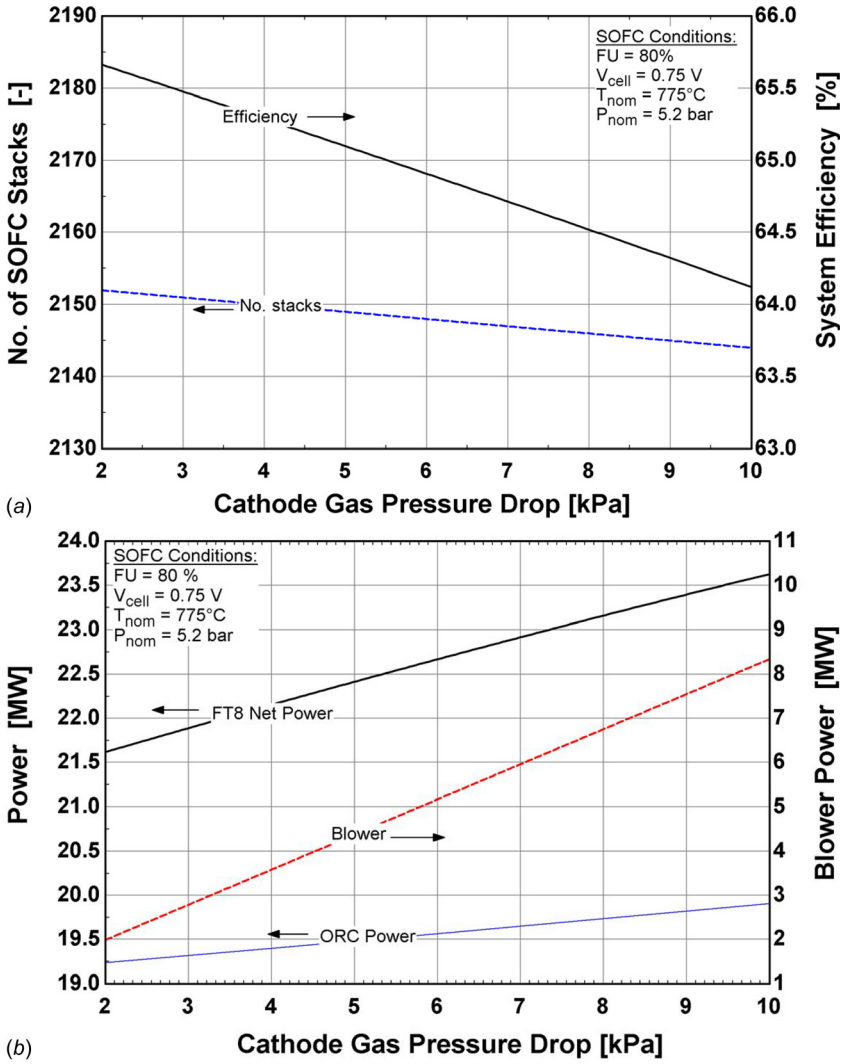

Fig. 10 Effect of cathode-side pressure drop on system parameters

results and trends of the study are constrained by the interactions between SOFC stack, gas turbine, and ORC subsystems. For example, an increase in SOFC efficiency via design operating cell voltage increase, results in a decrease of reactant gas flows to the gas turbine and thereby lowering its output power. Alternatively, enabling the means for fixing gas turbine flow via either supplemental syngas firing or utilizing nitrogen available from the ASU could provide improved net system performance. Additional considerations include (1) integrating the FT8 low-pressure compressor with the ASU, (2) syngas firing to maintain FT8 gas turbine inlet temperature as close to 950 °C as possible subject to 90% carbon capture constraints, (3) recuperation of syngas cleanup cooling loads to the ORC unit, and (4) examination of catalytic gasification technology which has as much as a 10 percentage point cold-gas efficiency advantage over entrained-flow gasification systems.

Nevetheless, the present study does reveal that entrained-flow gasifiers with oxycombustion system configurations can indeed lead to high power plant efficiencies. It also quantifies the effect of SOFC pressurization in the 3–5 bar range on system performance. It is worthwhile to note that these results have been obtained by using actual FT8 performance maps and SOFC performance based on near-term planar technology. In this study, a parametric sensitivity study was conducted on a given system configuration. It is not clear if the proposed system is the best possible design. However, the combined effect of selecting more "optimal" SOFC stack operating parameters, such as increasing cell voltage to 0.8V, cathode temperature rise to 150 °C, and decreasing per pass cell utilization (while maintaining overall fuel utilization) is expected to increase system performance by 3 percentage points or more.

7 Conclusions

This study detailed the performance of a 100 MW-scale IGFC hybrid power plant that integrated a pressurized SOFC power block with the low-pressure turbine spool of the Pratt & Whitney FT8-3 gas turbine and either a scaled-up, water-cooled version of the P&W PureCycle ORC or the larger P&W TurboDen product lines. The basic system concept included carbon capture via oxy-combustion followed by water knockout and CO_2 compression to pipeline ready CO_2 sequestration conditions. Performance results were reported that indicate hybrid SOFC systems could achieve electric efficiencies of 49% including CCS and as high as 67% when operating off a clean syngas and venting the CO_2 to the atmosphere. The impact of integrating an ORC bottoming cycle was found to add as much as 8 percentage points of efficiency to the system. Use of a steam power cycle, in lieu of the ORC, could increase net plant efficiency by another 3.7%. Additionally, the strategic use of gas expanders is particularly advantageous to offset carbon capture compression requirements or air separation unit parasitic power requirements.

A study of system performance sensitivity to a variation in SOFC design parameters revealed the strongest influences are design cell voltage, SOFC fuel utilization, and system pressure. The net system efficiency can vary by as much as 3 percentage

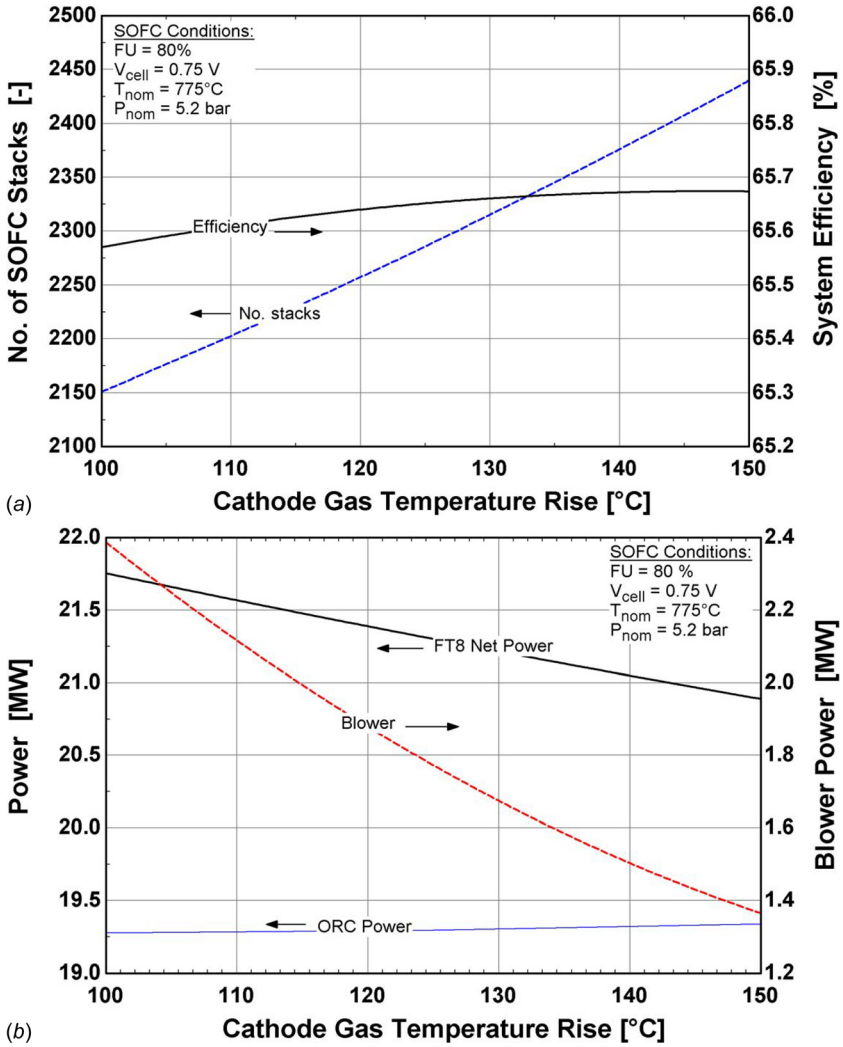

Fig. 11 Effect of stack ΔT on various system parameters in the hybrid IGFC system

points over the range studied for changes to any of these parameters. Anode tail gas recycle ratio and cathode side design parameters, such as pressure drop and temperature rise, only mildly affect system efficiency; however, increasing the recycle ratio of anode tail-gas has the negative effect of decreasing SOFC power density and hence, increasing the number of cell-stacks required. Depending on power density, two to three thousand SOFC stacks are required to generate 115 MW of dc power. Technoeconomic analysis could identify optimal stack design parameters.

It was also noted that additional analyses related to changes in the system design, such as ASU integration with the gas turbine or catalytic gasification could substantially improve the system performance beyond what is reported herein.

Acknowledgment

The authors would like to thank Pamela McNary, Bruce Wendus, and Joe Hilmon at Pratt & Whitney for their assistance in generating performance maps and engineering modifications to the FT8-3 gas turbine power system, and Lili Zhang at United Technologies Research Center for her helpful information on P&W PureCycle performance characteristics. This paper was prepared with the support of the U.S. Department of Energy, under Award Nos. DE-FC26-02NT41246 and DE-NT0005202. However, any opinions, finding, conclusions, or recommendations expressed herein are those of the authors and do not necessarily reflect the views of the DOE.

References

[1] Klara, J. M., 2009, "The Potential of Advanced Technologies to Reduce Carbon Capture Costs in Future IGCC Power Plants," Energy Procedia, **1**, 3827–3834.
[2] Santin, M., Traverso, A., and Massardo, A., 2008, "Technological Aspects of Gas Turbine and Fuel Cell Hybrid Systems for Aircraft: A Review," The Aeronaut. J., **112**(1134), pp. 459–467.
[3] Costamagna, P., Magistri, L., and Massardo, A., 2001, "Design and Part-Load Performance of a Hybrid System Based on a Solid Oxide Fuel Cell Reactor and a Micro Gas Turbine," J. Power Sources, **96**, 352–368.
[4] Roberts, R., Brouwer, J., Jabbari, F., Junker, T., and Ghezel-Ayagh, H., 2006, "Control Design of an Atmospheric Solid Oxide Fuel Cell/Gas Turbine Hybrid System: Variable Versus Fixed Speeed Gas Turbine Operation," J. Power Sources, **161**, 484–491.
[5] Traverso, A., Massardo, A., Roberts, R., Brouwer, J., and Samuelsen, S., 2007, "Gas Turbine Assessment for Air Management of Pressurized SOFC/GT Hybrid Systems," ASME J. Fuel Cell Sci. Technol., **4**, 373–383.
[6] Ferrari, M., 2011, "Solid Oxide Fuel Cell Hybrid System: Control Strategy for Stand-Alone Configurations," J. Power Sources, **196**, 2682–2690.
[7] Yang, J. S., Sohn, J. L., and Ro, J., 2007, "Performance Characteristics of a Solid Oxide Fuel Cell/Gas Turbine Hybrid System With Various Part-Load Control Modes," J. Power Sources, **166**, 155–164.
[8] Mueller, F., Gaynor, R., Auld, A., Brouwer, J., Jabbari, F., and Samuelsen, G., 2008, "Synergistic Integration of a Gas Turbine and Solid Oxide Fuel Cell for Improved Transient Capability," J. Power Sources, **176**, 229–239.
[9] Tucker, D. Lawson, L., and Gemmen, R., 2005, "Characterisation of Air Flow Management and Control in a Fuel Cell Turbine Hybrid Power System Using Hardware Simulation," ASME Paper No. PWR2005-50127.
[10] Research and Development Solutions, LLC, 2007, "Cost and Performance Baseline for Fossil Energy Plants," Final Report, U.S. DOE, National Energy Technology Laboratory, DOE/NETL-2007/1281, August, Vol. 1.
[11] Lobachyov, K., and Richter, H. J., 1996, "Combined Cycle Gas Turbine Power Plant With Coal Gasification and Solid Oxide Fuel Cell," J. Energy Res. Technol., **118**, 285–292.

[12] Kivisaari., T., Björnbom, P., Sylwan, C., Jacquinot, B., Jansen, D., and de Groot, A., 2004, Chem. Eng. J., 100, 167–180.
[13] Ghosh, S., and De, S., 2006, "Energy Analysis of a Cogeneration Plant Using Coal Gasification and Solid Oxide Fuel Cell," Energy, **3**, 345–363.
[14] Verma, A., Rao, A. D., and Samuelsen, G.S., 2006, "Sensitivity Analysis of a Vision 21 Coal Based Zero Emission Power Plant," J. Power Sources, **158**, 417–427.
[15] Romano, M., Campanari, S., Spallina, V., and Lozza, G., 2009, "SOFC-Based Hybrid Cycle Integrated With a Coal Gasification Plant," ASME Paper No. GT2009-59551.
[16] Liese, E., 2010, "Comparison of Preanode and Postanode Carbon Dioxide Separation for IGFC Systems," ASME J. Eng. Gas Turbines Power, **132**, 061703.
[17] Siefert, N., Shekhawat, D., and Kalapos, T., 2010, "Integrating Catalytic Coal Gasifiers With Solid Oxide Fuel Cells," ASME Paper No. FC2010-33206.
[18] Gerdes, K., Grol, E., Keairns, D., and Newby, R., 2009, "Integrated Gasification Fuel Cell Performance and Cost Assessment," Report No. DOE/NETL-2009/1361, March, National Energy Technology Laboratory, Morgantown, WV.
[19] Verda, V., 2008, "Solid Oxide Fuel Cell System Configurations for Distributed Generation," ASME J. Fuel Cell Sci. Technol., **5**, 041001.
[20] Shelton, W., and Lyons, J., 2000, "Shell Gasifier IGCC Base Cases," PED-IGCC-98-002, revised, prepared by EG&G for the U.S. Department of Energy, Office of Fossil Energy, National Energy Technology Laboratory, Morgantown, WV.
[21] Pratt & Whitney Power Systems, 2010, "Organic Rankine Cycle Technology," product brochure, PS-S0022.01.10, available from www.pw.utc.com
[22] Process Systems Enterprise, Ltd., 2009, http://www.psenterprise.com/gproms/index.html, as accessed on 11/2015/2006.
[23] Simbeck, D. R., Korens, N., Biasca, F. E., Vejtasa, S., and Dickenson, R. L., 1993, "Coal Gasification Guidebook: Status, Applications, and Technologies," Electric Power Research Institute Final Report No. TR-102034, Palo Alto, CA.
[24] Chiesa, P., Consonni, S., Kreutz, T., and Williams, R., 2005, Int. J. Hydrogen Energy, **30**, 747–767.
[25] West Virginia University Chemical Engineering Department, 2009, "Large-Scale Process Design Projects: Air Separation Into Oxygen, Nitrogen and Argon," http://www.che.cemr.wvu.edu/publications/projects/large_proj/air.PDF, accessed June 1.
[26] American Water Works Association, 1997, *Water Treatment Plant Design*, 3rd ed., American Society of Civil Engineers/McGraw Hill, New York.
[27] USDE, 2008, Proceedings of the 9th Annual Solid State Energy Conversion Alliance (SECA) Workshop, U.S. Department of Energy, National Energy Technology Laboratory, August 5–7.
[28] Williford, R. E., Chick, L. A., Maupin, G. D., Simner, S. P., and Stevenson, J.W., 2003, J. Electrochem. Soc., **150**(8), A1067–A1072.
[29] Pratt & Whitney Power Systems, 2010, "Organic Rankine Cycle Technology," Product Brochure (PS-S0022.01.10), www.pw.utc.com
[30] GE Power, 2008, "GE Combined Cycle Product Line and Performance," GE Power Product and Services Website Information, Publication document No. GER3574g.
[31] Farmer, R., ed., 2006, *Gas Turbine World Handbook*, Pequot, Southport, CT.
[32] U.S. DOE, 2005, "Carbon Capture and Sequestration Systems Analysis Guidelines," Office of Fossil Energy, NETL, April.
[33] Probstein, R. F., and Hicks, R.E., 2006, *Synthetic Fuels*, Dover, Mineola, NY.
[34] Marsano, F., Magistri, L., and Massardo, A., 2004, "Ejector Performance Influence on a Solid Oxide Fuel Cell Anodic Recirculation System," J. Power Sources, **129**, 216–228.
[35] Wilson, D. G., 2003, "Regenerative Heat Exchangers for Microturbines, and an Improved Type," Proceedings of the ASME Turbo Expo 2003, June 16–19, Atlanta, Georgia.
[36] EG&G Technical Services, Inc., 2004, *Fuel Cell Handbook*, 7th ed., prepared for the U.S. DOE Office of Fossil Energy, National Energy Technology Laboratory, Morgantown, WV.
[37] Braun, R. J., 2010, "Techno-Economic Optimal Design of Solid Oxide Fuel Cell Systems for Micro-Combined Heat and Power Applications in the U.S.," ASME J. Fuel Cell Sci. Technol. **7**, p. 031018.